Hindawi Publishing Corporation
Advances in High Energy Physics
Volume 2014, Article ID 731864, 6 pages
http://dx.doi.org/10.1155/2014/731864

Research Article

Transverse Momentum Distributions in AuAu and dAu Collisions at $\sqrt{s_{NN}} = 200$ GeV

Li-Li Wang

Department of Mathematics, Business College of Shanxi University, Taiyuan, Shanxi 030031, China

Correspondence should be addressed to Li-Li Wang; llwang2007@163.com

Received 24 January 2014; Revised 18 March 2014; Accepted 24 March 2014; Published 10 April 2014

Academic Editor: Chen Wu

We study the transverse momentum distributions of identified particles produced in Au + Au and d + Au collisions at $\sqrt{S_{NN}}$ = 200 GeV. The Tsallis description is applied in the multisource model. The results are compared with the experimental data in detail. We obtain some information of the thermodynamic properties of matter produced in the collisions. The difference of the transverse momentum distributions in Au + Au and d + Au collisions is not significant.

1. Introduction

Nucleus-nucleus collisions at high energy are important experiments to study the matter at an extreme temperature. Relativistic heavy ion collider (RHIC) in Brookhaven National Laboratory (BNL) is a valuable tool to probe quark-gluon plasma (QGP) produced in the collisions. In order to understand QGP more deeply, scientists have built a large hadron collider (LHC) at the European Organization for Nuclear Research (CERN). In the high-energy collisions, thousands of final-state particles are produced per event. The investigation of the identified particles produced in the collisions brings valuable insight into properties of QGP. In Au + Au collisions, final-state particle yields provided the information of the temperature T and chemical potential μ by using a statistical model [1]. The transverse momentum of a particle is defined as $p_T = \sqrt{p_x^2 + p_y^2}$, where p_x and p_y are the momentum components in the transverse momentum plane. The transverse momentum distributions of the final-state particles are called first observations in the high-energy experiments. To describe such many-particle system, statistical approaches have been used widely over past few years.

In order to describe transverse momentum spectra of the identified particles, the Tsallis statistics have been utilized to understand the particle production in high-energy physics and have been used to describe the transverse momentum spectra measured at the RHIC [2] and at the LHC [3, 4]. By the analysis of the experimental data, the Tsallis distribution has gained prominence with very good descriptions. Recently, the Tsallis distribution was improved to satisfy the thermodynamic consistence in the case of relativistic high-energy quantum distribution [5]. By fitting the data observed at LHC, the temperature T and the parameter q have been estimated. One-particle rapidity (or pseudorapidity) distributions measured at RHIC are well described by the Ornstein-Uhlenbeck process [6, 7].

In our previous work [8], inclusive transverse momentum spectra of η meson in Au-Au, d-Au, and p-p collisions were studied in the framework of a thermalized cylinder model. In the region of high transverse momentum, the considered distributions of η meson have a tail part at the maximum energy of RHIC. To explain the wider transverse momentum spectra, we considered the relative importance of hard and soft processes in the particle production. The experimental data of the PHENIX Collaboration have been described by the improved cylinder model, which contains two fundamental components. The multisource thermal model was developed from the cylinder model [9–11]. In this paper, we consider the different longitudinal rapidity of emission sources produced in Au + Au and d + Au collisions at $\sqrt{s_{NN}}$ = 200 GeV and extend the one-source Tsallis distribution to

the multisource Tsallis distribution in the picture of the multisource thermal model.

2. The Distribution Law of Particles Produced in AuAu and dAu Collisions at 200 GeV

At high energy, the primary nucleon-nucleon collision may be treated as a few sources. The participant nucleons in the primary collisions have probabilities to collide with latter nucleons in cascade collisions. Furthermore, the particles produced in primary or cascade nucleon-nucleon collisions have probabilities to take part in secondary collisions with latter nucleons and other particles. Each cascade or secondary collision is also treated as an emission source or a few emission sources. The identified particles are emitted from the emission sources produced in Au + Au and d + Au collisions at RHIC. According to the improved Tsallis distribution [5], the total number of the particles is

$$N = gV \int \frac{d^3P}{(2\pi)^3}\left[1 + (q-1)\,\frac{E-\mu}{T}\right]^{-q/(q-1)}, \quad (1)$$

where p, E, T, μ, V, and g are the momentum, the energy, the temperature, the chemical potential, the volume, and the degeneracy factor, respectively. The parameter q characterizes the degree of nonequilibrium. Then, we have momentum distribution

$$E\frac{d^3N}{d^3P} = \frac{gVE}{(2\pi)^3}\left[1 + (q-1)\,\frac{E-\mu}{T}\right]^{-q/(q-1)}. \quad (2)$$

At midrapidity $y = 0$, for zero chemical potential, the transverse momentum spectrum is given by

$$\left.\frac{d^2N}{p_T dp_T dy}\right|_{y=0} = \frac{gVm_T}{(2\pi)^2}\left[1 + (q-1)\,\frac{m_T}{T}\right]^{-1/(q-1)}. \quad (3)$$

The p_T distribution of the particles is contributed by an emission source at midrapidity $y = 0$. Considering the contributions of the sources at the different rapidities [13], the p_T spectrum is

$$\frac{dN}{p_T dp_T} = \frac{gV}{(2\pi)^2}\int_{y_{\min}}^{y_{\max}} \cosh y dy m_T \times \left[1 + (q-1)\frac{m_T \cosh y}{T}\right]^{-q/(q-1)}. \quad (4)$$

Figure 1 shows the invariant yields of positive pions and negative pions as a function of the transverse momentum for 0–10%, 10–20%, 20–40%, 40–60%, and 60–92% centralities in Au + Au collisions and for 0–20%, 20–40%, 0–100%, 40–60%, and 60–88% centralities in d + Au collisions at $\sqrt{s_{NN}}$ = 200 GeV. The scattered symbols denote the experimental data measured by the PHENIX Collaboration [12]. The yields are scaled by arbitrary factors indicated in the figure for the sake of clarity and for keeping the collision species grouped together. The lines are the results calculated by the model. The parameters T and q used in the calculations and the corresponding χ^2/dof are given in Table 1. The maximum χ^2/dof is 0.495. Our results of π^+ and π^- are in good agreement with the experimental data for all concerned centralities. The values of the temperature T increase slowly with increasing the centrality. The q does not change significantly. In both Au + Au and d + Au, the trends of T and q are the same.

In Figure 2, we show the transverse momentum spectra of positive kaons and negative kaons in Au + Au and d + Au collisions at $\sqrt{s_{NN}}$ = 200 GeV. The scattered symbols denote the experimental data measured by the PHENIX Collaboration [12] and the solid lines are the results calculated by the formula of the multisource thermal model. The parameters T and q are given in Table 2 with the corresponding χ^2/dof. The mass of the kaon is heavier than that of the poin. But, for K^+ and K^- with all concerned centralities, our results are also in good agreement with the experimental data. The maximum χ^2/dof is 0.425. Similarly, the values of the temperature T increase slowly with the centrality and the parameter q hardly changes in both Au + Au and d + Au collisions.

Figure 3 presents the invariant yields of protons and negative protons for 0–10%, 10–20%, 20–40%, 40–60%, and 60–92% centralities in Au + Au collisions and for 0–20%, 20–40%, 0–100%, 40–60%, and 60–88% centralities in d + Au collisions at $\sqrt{s_{NN}}$ = 200 GeV. The scattered symbols denote the experimental data [12] in different centrality cuts indicated in the figure. The solid lines are our results calculated by the model. The parameters T and q are given in Table 3 with χ^2/dof. The range of χ^2/dof is 0.151–1.440. Therefore, the model can approximately describe the experimental data of p and $\overline{p}$ for all concerned centralities in Au + Au and d + Au systems. It is also found that the temperature T increases slowly with increasing the centrality and the q does not change significantly in both Au + Au and d + Au collisions.

3. Conclusions

We have studied the invariant yields of π^+, π^-, K^+, K^-, p, and $\overline{p}$ produced in Au + Au and d + Au collisions at $\sqrt{s_{NN}}$ = 200 GeV in the framework of the multisource model, which is combined with Tsallis statistics. A formula was introduced to describe the transverse momentum distributions and to obtain q and the temperature T. For the two collision systems Au + Au and d + Au at high energy, the mechanism of the particle production has the commonality of their inherent and fundamental laws. So the identified particles can be described in the same model. In recent years, the particle production in high-energy ion collisions has attracted much attention to understand the strongly coupled QGP (sQGP) by analyzing the production mechanisms [14, 15]. Thermal-statistical models have succeeded in the description of particle yields in various collision systems at different energies [10, 11, 16]. In the rapidity space, different sources of final-state particles stay at different positions due to stronger longitudinal flow [17].

In our previous work, the transverse momentum distributions of η meson in Au + Au, d + Au, and p + p collisions were investigated in the framework of a thermalized cylinder model. There is a tail part in the transverse momentum distributions of η mesons at RHIC energies.

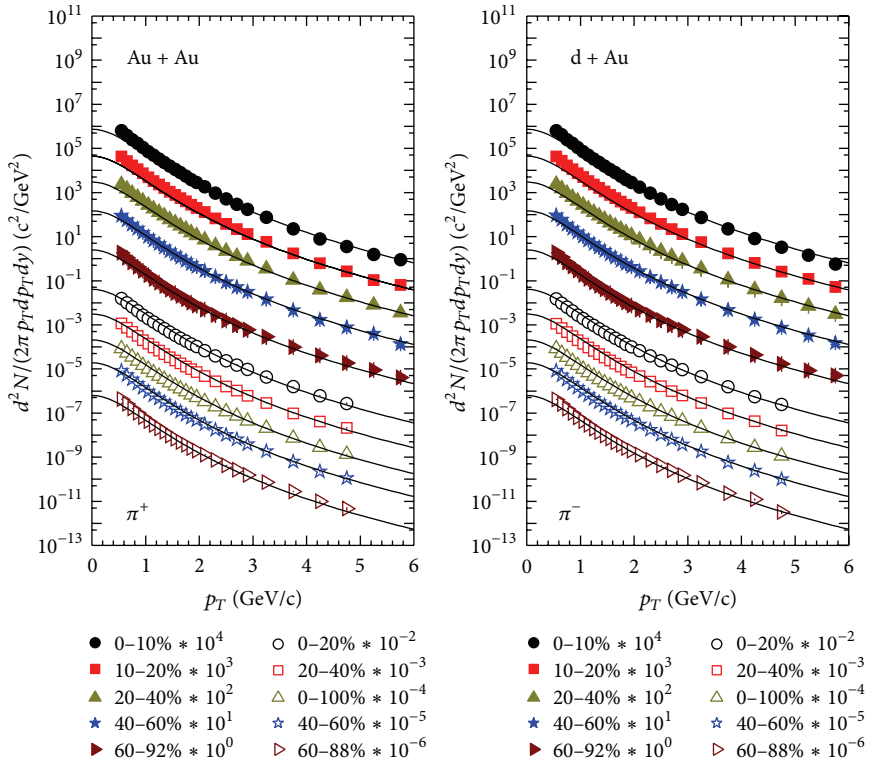

FIGURE 1: Invariant yield of π^+ and π^- as a function of p_T in Au + Au and d + Au collisions at $\sqrt{s_{NN}}$ = 200 GeV. The scattered symbols denote the experimental data measured by the PHENIX Collaboration [12] and statistical uncertainties are too small to be seen. The solid lines denote the results of the model.

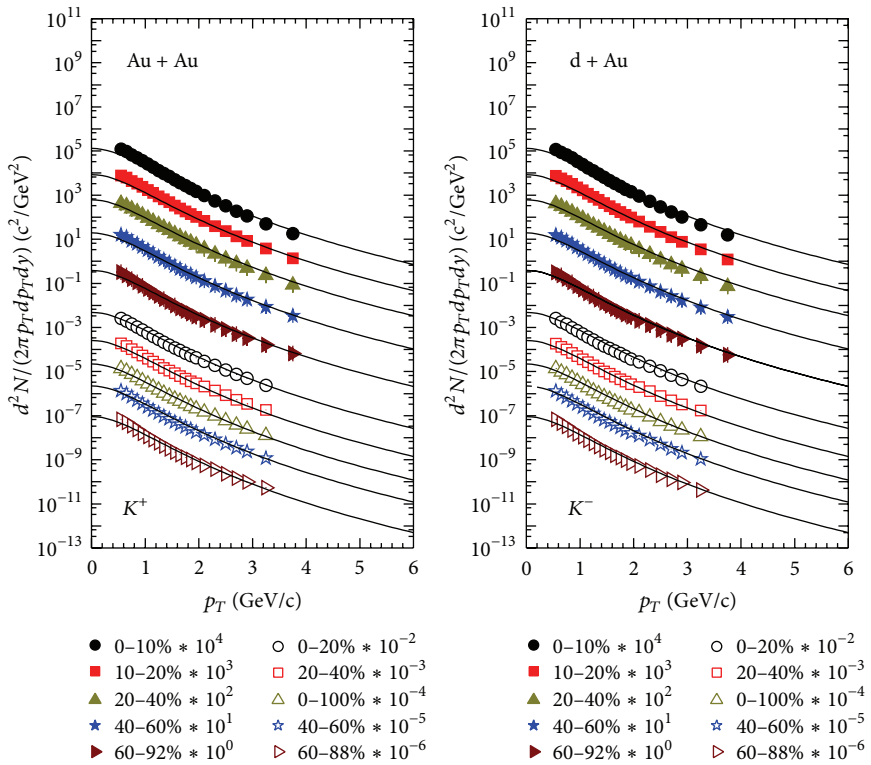

FIGURE 2: Invariant yield of K^+ and K^- as a function of p_T in Au + Au and d + Au collisions at $\sqrt{s_{NN}}$ = 200 GeV. The scattered symbols denote the experimental data measured by the PHENIX Collaboration [12] and statistical uncertainties are too small to be seen. The solid lines denote the results of the model.

Table 1: The parameters T and q in Figure 1.

Particles	Collision	Centralities	q	T (GeV)	χ^2/dof
π^+	Au + Au	02–10%	1.110	0.752	0.427
		10–20%	1.107	0.722	0.415
		20–40%	1.105	0.705	0.402
		40–60%	1.108	0.688	0.257
		60–92%	1.104	0.664	0.275
	d + Au	0–20%	1.105	0.725	0.201
		20–40%	1.104	0.681	0.158
		0–100%	1.102	0.661	0.115
		40–60%	1.103	0.666	0.145
		60–88%	1.097	0.640	0.181
π^-	Au + Au	0–10%	1.110	0.746	0.457
		10–20%	1.107	0.729	0.495
		20–40%	1.105	0.717	0.416
		40–60%	1.108	0.702	0.261
		60–92%	1.104	0.684	0.285
	d + Au	0–20%	1.105	0.721	0.109
		20–40%	1.104	0.678	0.090
		0–100%	1.102	0.658	0.116
		40–60%	1.103	0.662	0.125
		60–88%	1.097	0.635	0.140

Table 2: The parameters T and q in Figure 2.

Particles	Collision	Centralities	q	T (GeV)	χ^2/dof
K^+	Au + Au	0–10%	1.105	0.108	0.392
		10–20%	1.102	0.104	0.416
		20–40%	1.103	0.098	0.240
		40–60%	1.106	0.095	0.156
		60–92%	1.101	0.091	0.275
	d + Au	0–20%	1.104	0.103	0.212
		20–40%	1.101	0.096	0.122
		0–100%	1.102	0.090	0.165
		40–60%	1.100	0.092	0.245
		60–88%	1.101	0.085	0.401
K^-	Au + Au	0–10%	1.105	0.107	0.425
		10–20%	1.102	0.102	0.355
		20–40%	1.103	0.097	0.314
		40–60%	1.106	0.094	0.275
		60–92%	1.101	0.091	0.418
	d + Au	0–20%	1.104	0.101	0.217
		20–40%	1.101	0.095	0.142
		0–100%	1.102	0.087	0.175
		40–60%	1.100	0.088	0.215
		60–88%	1.101	0.081	0.375

To explain the wider transverse momentum spectra, the hard and soft processes have been taken into account in the particle production. The improved cylinder model with two-component distribution is successful in the description of the meson production. But we can only obtain an indirect association with the temperature of the emission sources. The multisource thermal model was improved from the cylinder model. In this paper, we consider the different longitudinal rapidity of the emission sources created in Au + Au and d + Au collisions at $\sqrt{s_{NN}}$ = 200 GeV and extend

Table 3: The parameters T and q in Figure 3.

Particles	Collision	Centralities	q	T (GeV)	χ^2/dof
p	Au + Au	0–10%	1.115	0.120	0.786
		10–20%	1.114	0.118	0.951
		20–40%	1.115	0.115	1.440
		40–60%	1.112	0.111	0.658
		60–92%	1.114	0.108	0.524
	d + Au	0–20%	1.112	0.116	0.540
		20–40%	1.110	0.112	0.415
		0–100%	1.110	0.109	0.400
		40–60%	1.111	0.106	0.341
		60–88%	1.109	0.102	0.375
$\bar{p}$	Au + Au	0–10%	1.115	0.119	0.495
		10–20%	1.114	0.117	0.575
		20–40%	1.115	0.114	0.501
		40–60%	1.112	0.111	0.425
		60–92%	1.114	0.106	0.261
	d + Au	0–20%	1.112	0.114	0.245
		20–40%	1.110	0.111	0.224
		0–100%	1.110	0.107	0.217
		40–60%	1.111	0.105	0.174
		60–88%	1.109	0.101	0.151

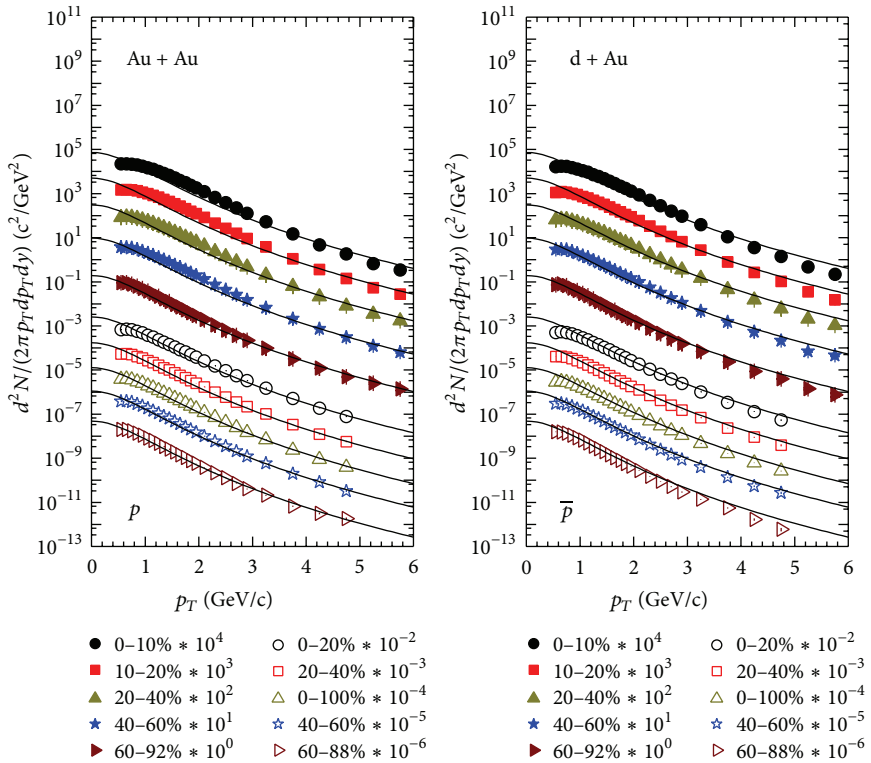

Figure 3: Invariant yield of p and $\overline{p}$ as a function of p_T in Au + Au and d + Au collisions at 200 GeV. The scattered symbols denote the data measured by the PHENIX Collaboration [12] and statistical uncertainties are too small to be seen. The solid lines denote the results of the model.

the improved Tsallis distribution with one source to the Tsallis distribution with multisource in the picture of the multisource thermal model. The relativistic treatment for the transverse direction would be needed as long as the stochastic approach is adopted. Our results are in agreement with the experimental data of PHENIX Collaboration. Even more important, the model can quantitatively provide the temperature information of the emission sources.

Conflict of Interests

The author declares that there is no conflict of interests regarding the publication of this paper.

Acknowledgments

The author would like to thank Dr. J. H. Kang for her guidance throughout the work. The author thanks also Dr. B. C. Li for his improvements to the paper.

References

[1] J. Adams, C. Adler, M. M. Aggarwal et al., "Identified particle distributions in pp and Au+Au Collisions at $\sqrt{S_{NN}}$ = 200 GeV," *Physical Review Letters*, vol. 92, Article ID 112301, 2004.

[2] A. Adare, S. Afanasiev, C. Aidala et al., "Identified charged hadron production in $p + p$ collisions at $\sqrt{s} = 200$ and 62.4 GeV ," *Physical Review C*, vol. 83, Article ID 064903, 2011.

[3] V. Khachatryan, A. M. Sirunyan, A. Tumasyan et al., "Strange particle production in pp collisions at $\sqrt{S} = 0.9$ and 7 TeV," *Journal of High Energy Physics*, vol. 1105, article 064, 2011.

[4] G. Aad, B. Abbott, J. Abdallah et al., "Charged-particle multiplicities in pp interactions measured with the ATLAS detector at the LHC," *New Journal of Physics*, vol. 13, Article ID 053033, 68 pages, 2011.

[5] J. Cleymans and D. Worku, "The Tsallis distribution in proton–proton collisions at $\sqrt{s} = 0.9$ TeV at the LHC ," *Journal of Physics G: Nuclear and Particle Physics*, vol. 39, Article ID 025006, 2012.

[6] G. Wolschin, "Diffusion and local deconfinement in relativistic systems," *Physical Review C*, vol. 69, Article ID 024906, 2004.

[7] N. Suzuki and M. Biyajima, "Transverse momentum distribution with radial flow in relativistic diffusion model," *International Journal of Modern Physics E*, vol. 16, p. 133, 2007.

[8] L.-L. Wang, "Emission of η meson with high transverse momentum in Au-Au, d-Au and p-p collisions at TeX GeV," *Indian Journal of Physics*, vol. 87, no. 6, pp. 575–579, 2013.

[9] B.-C. Li, Y.-Z. Wang, and E.-Q. Wang, "Meson production in high energy p+p collisions at the RHIC energies," *Advances in High Energy Physics*, vol. 2013, Article ID 486476, 7 pages, 2013.

[10] B.-C. Li, Y. Fu, L.-L. Wang, and F.-H. Liu, "Dependence of elliptic flows on transverse momentum and number of participants in Au+Au collisions at $\sqrt{S_{NN}}$ = 200 GeV," *Journal of Physics G: Nuclear and Particle Physics*, vol. 40, no. 2, Article ID 025104, 2013.

[11] F.-H. Liu, C.-X. Tian, M.-Y. Duan, and B.-C. Li, "Relativistic and quantum revisions of the multisource thermal model in high-energy collisions," *Advances in High Energy Physics*, vol. 2012, Article ID 287521, 9 pages, 2012.

[12] A. Adare, S. Afanasiev, C. Aidala et al., "Spectra and ratios of identified particles in Au+Au and d+Au collisions at $\sqrt{S_{NN}}$ = 200 GeV ," *Physical Review C*, vol. 88, Article ID 024906, 2013.

[13] B. C. Li, Y. Z. Wang, F. H. Liu, X. J. Wen, and Y. E. Dong, "Particle production in relativistic $pp(\overline{p})$ collisions at RHIC and LHC energies with Tsallis statistics using the two-cylindrical multisource thermal model," *Physical Review D*, vol. 89, Article ID 054014, 2014.

[14] A. Adare, S. Afanasiev, C. Aidala et al., "Azimuthal anisotropy of π^0 and η mesons in Au + Au collisions at $\sqrt{S_{NN}}$ = 200 GeV," *Physical Review C*, vol. 88, Article ID 064910, 2013.

[15] B. B. Abelev, J. Adam, D. Adamova et al., "K^0_S and Λ Production in Pb-Pb Collisions at $\sqrt{S_{NN}} = 200$ TeV ," *Physical Review Letters*, vol. 111, Article ID 222301, 2013.

[16] B.-C. Li, Y.-Z. Wang, and F.-H. Liu, "Formulation of transverse mass distributions in Au–Au collisions at $\sqrt{S_{NN}} = 200$ GeV/nucleon," *Physics Letters B*, vol. 725, no. 4-5, pp. 352–356, 2013.

[17] P. Braun-Munzinger, J. Stachel, J. P. Wessels, and N. Xu, "Thermal equilibration and expansion in nucleus-nucleus collisions at the AGS," *Physics Letters B: Nuclear, Elementary Particle and High-Energy Physics*, vol. 344, pp. 43–48, 1995.